Asymptotic stress fields for complete contact between dissimilar materials

Kisik Hong*
Department of Mechanical Engineering
University of Michigan
Ann Arbor, MI 48109-2125
Email: kisik@umich.edu

M. D. Thouless
Professor
Department of Mechanical Engineering
Department of Materials Science & Engineering
University of Michigan
Ann Arbor, MI 48109-2125
Email: thouless@umich.edu

Wei Lu
Professor
Department of Mechanical Engineering
University of Michigan
Ann Arbor, MI 48109-2125
Email: weilu@umich.edu

J. R. Barber
Professor
Department of Mechanical Engineering
University of Michigan
Ann Arbor, MI 48109-2125
Email: jbarber@umich.edu

ABSTRACT

We investigate the influence of material dissimilarity on the traction fields at the corners of a contact between an elastic right-angle wedge and an elastic half-plane. The local asymptotic fields are characterized in terms of the properties of the leading eigenvalue for cases of slip and stick as a function of the Dundurs bimaterial parameters α *and* β*, and the coefficient of friction* f*. Permissible values of* α *and* β *are partitioned into two possible ranges, one where behaviour is qualitatively similar to the case where the indenting wedge is rigid [*$\alpha = 1$*], and one where behaviour is similar to the case where the materials are the same [*$\alpha = \beta = 0$*]. The results give insight into the high local stresses at the edge of a contact between elastically dissimilar bodies, and can also be used to evaluate the effectiveness of mesh refinement in corresponding finite-element models.*

*Corresponding author.

1 Introduction

If an elastic body with a sharp corner is pressed against an elastic half-plane, the stress field near the corner can be characterized by an asymptotic or eigenfunction series

$$\sigma_{ij}(r,\theta) = \sum_{n=1}^{\infty} K_n r^{\lambda_n - 1} f_{ij}^n(\theta) \tag{1}$$

[1], where the coordinate system (r,θ) is defined in Fig. 1(a), and the constants K_n [often called 'generalized stress-intensity factors'] depend on the far-field loading of the bodies. The eigenvalues, λ_n, and the corresponding eigenfunctions, $f_{ij}^n(\theta)$, are obtained by considering a single term of the series, and solving the resulting elasticity problem with traction-free conditions at the exposed edges and appropriate contact conditions at the interface $\theta = 0$.

Energetic considerations restrict admissible eigenvalues to the range $\lambda_n > 0$, or if complex, $\Re(\lambda_n) > 0$. Conventionally, the eigenvalues are arranged in order of ascending real part, so the stress field very near the corner is dominated by the first term in equation (1). In particular, if a quarter-plane is pressed onto a half-plane as shown in Fig. 1(a), the frictional [shear] traction $q(r)$ and the contact pressure $p(r)$ near the corner can be approximated as

$$\begin{aligned} p(r) &= -\sigma_{\theta\theta}(r,0) \approx -K_1 r^{\lambda_1 - 1} f_{\theta\theta}^1(0); \\ q(r) &= \sigma_{\theta r}(r,0) \approx K_1 r^{\lambda_1 - 1} f_{\theta r}^1(0), \end{aligned} \tag{2}$$

where the sign convention for p and q is shown in Fig. 1(b). Important features of the contact problem can often be deduced by considering this term alone [2]. We define the eigenfunctions such that $f_{\theta\theta}^1(0) > 0$, so the unilateral contact condition $p > 0$ is satisfied only for $K_1 < 0$. This is in accordance with the sign convention used in fracture mechanics.

The form of the eigenfunction series (1) depends on whether or not interface slip occurs near the edge. We shall identify the two cases by the superscripts $^{(s)}$ [slip] and $^{(a)}$ [adhered] respectively. In the case of slip, $q = \pm fp$ where f is the friction coefficient, and the sign depends on the direction of slip. The motion is described as *trailing-edge slip* if body 2 moves to the right in Fig. 1(b), and *leading-edge slip* if it moves to the left [3]. The frictional tractions must oppose the slip motion, and hence, $q > 0$ at a trailing edge and $q < 0$ at a leading edge. These inequalities can be used to characterize the edge conditions even in the case where there is no slip. It must be emphasized that this terminology relates to asymptotic conditions at the corner, and is not necessarily connected to the macroscopic conditions of the problem. For example, if a rectangular block is pressed against a half-plane and then subjected to normal and shear loads P, Q respectively, it might seem more natural to define leading and trailing edges with reference to the direction of Q. However, the asymptotic arguments presented here can be applied to more complex geometries where such a definition would be impractical.

If there is no slip at the edge, the ratio of the shear and normal tractions in the K_1-dominated zone is defined by

$$\frac{q(r)}{p(r)} = -f_a \quad \text{where} \quad f_a = \frac{f_{\theta r}^{1(a)}(0)}{f_{\theta\theta}^{1(a)}(0)} \tag{3}$$

and is independent of $K_1^{(a)}$ and r. Churchman and Hills [2] showed that $f_a = 0.543$ for the case where the materials have the same elastic properties and argued that if the coefficient of friction at the interface $f > f_a$ there can be no slip in the corner [*regardless of the far-field loading or geometry*]. If $K_1^{(a)} > 0$, the corner must separate, whereas if $K_1^{(a)} < 0$, it will be in contact with no slip and the shear traction $q < 0$ in Fig. 1(b), which by the above convention defines a leading edge. By contrast, if $f < f_a$, 'stick' is impossible, and the corner must either slip or separate.

Further information about the local fields can be obtained by including the second term in the asymptotic series (1). Since $\lambda_1^{(a)} \neq \lambda_2^{(a)}$, the constants $K_1^{(a)}, K_2^{(a)}$ involve different dimensions of length and hence we can define a problem-specific length scale

$$d_0 = \left(\frac{K_1^{(a)}}{K_2^{(a)}} \right)^{1/(\lambda_2^{(a)} - \lambda_1^{(a)})} \tag{4}$$

[4]. This gives some indication of the range $r < d_0$ in which the first term in the series is likely to be dominant, but in partial slip problems with $f < f_a$, it also allows us to estimate the length of the slip zone at the edge of the contact, as a multiple of

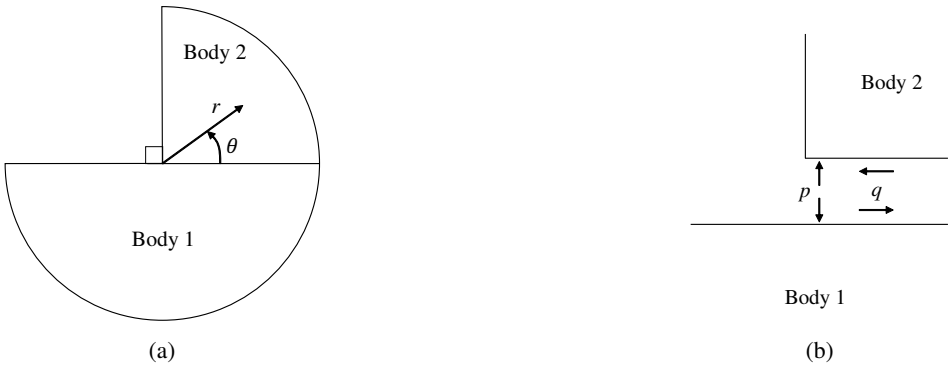

Fig. 1: (a) A quarter-plane [right-angle wedge] indenting a half-plane. (b) Sign convention for normal traction p and shear traction q. At a trailing edge, $q = fp$ and at a leading edge, $q = -fp$.

d_0, that depends only on the coefficient of friction [4]. Many of these results were extended to the case of dissimilar materials by Kim *et al.* [5].

Notice that these effects are typically characterized by the adhered asymptotic series, even in cases where stick is impossible in the corner. In that case, we anticipate the existence of a $K_1^{(a)}$-dominated zone *away* from the edge, with an embedded corner zone involving slip and/or separation, whose properties are determined by the first two terms of the surrounding asymptotic series. The situation is analogous to that in LEFM, where we anticipate a small region of non-linear deformation near the crack tip whose characteristics are determined by the mode I and mode II stress-intensity factors.

If slip extends to the corner, the local field (1) will be determined by the slip asymptotic, with the leading term defining the tractions as

$$\begin{aligned} p(r) &\approx -K_1^{(s)} r^{\lambda_1^{(s)}-1}; \\ q(r) &\approx \pm f K_1^{(s)} r^{\lambda_1^{(s)}-1}, \end{aligned} \tag{5}$$

where the sign depends on the direction of slip. Here, we have chosen to normalize the eigenfunctions such that $f_{\theta\theta}^{1(s)}(0) = 1$. Karuppanan *et al.* [3] considered the case where an elastic block slides over a half-plane, so that $q = \pm fp$ in any contact zone. For the trailing edge, they identified two critical friction coefficients, f_b and f_c, such that for $f < f_b$, the first 'slip' eigenvalue $\lambda_1^{(s)} < 1$ and hence the asymptotic stress field is singular, whereas for $f_b < f < f_c$, $\lambda_1^{(s)} > 1$ and the field is bounded, with stresses and tractions tending to zero in the corner. For $f > f_c$ [$> f_b$], $\lambda_1^{(s)}$ becomes complex, implying oscillatory tractions near the corner. There will then exist regions where the contact pressure is negative, which violates the Signorini contact inequalities. It was argued that this implies slip at the trailing edge is impossible, and, therefore, a small region near the trailing edge must separate. Karuppanan *et al.* [3] verified this by solving the edge contact problem under unilateral conditions, using a distribution of climb and glide dislocations to model the displacement discontinuities. Also, finite-element studies of particular contact problems confirm these conclusions.

At a leading edge, the first eigenvalue $\lambda_1^{(s)}$ is real for all friction coefficients and defines a singular stress field. However, if $f > f_a$ [defined in equation (3)], leading-edge slip can only occur under gross-slip [sliding] conditions. For contacts involving partial slip, a leading edge must either stick or separate if $f > f_a$.

Except for [5], the above studies were all restricted to the case of elastically similar materials, but, in practice, complete contact problems are frequently encountered between engineering components with different elastic properties. For example, in nuclear reactors a complete contact can occur between a fragmented fuel pellet and cladding during a power transient [6]. This induces high tensile hoop stresses at the contact edges, leading to a pellet-cladding interaction (PCI) failure. In the present paper, we therefore propose to examine the effect of elastic mismatch on the nature of the eigenvalues in equation (1) and on the critical coefficients of friction f_a, f_b, f_c. Hence, we can anticipate the qualitative behaviour of a contact edge under both partial-slip and gross-slip conditions.

2 Asymptotic analysis

Plane-strain contact problems involving dissimilar materials are most efficiently characterized in terms of the Dundurs bimaterial parameters, α and β, defined as

$$\begin{aligned}\alpha &= E^* \left[\frac{(1-\nu_1)}{2G_1} - \frac{(1-\nu_2)}{2G_2} \right] ; \\ \beta &= E^* \left[\frac{(1-2\nu_1)}{4G_1} - \frac{(1-2\nu_2)}{4G_2} \right] \end{aligned} \tag{6}$$

[7], where G, ν denote the shear modulus and Poisson's ratio respectively, the indices refer to the materials of bodies 1 and 2 in Fig. 1, and the contact modulus E^* is defined such that

$$\frac{1}{E^*} = \frac{(1-\nu_1)}{2G_1} + \frac{(1-\nu_2)}{2G_2} \, . \tag{7}$$

With this notation, the characteristic equation defining the eigenvalues $\lambda_i^{(s)}$ for the slipping interface is [8, 9]

$$\begin{aligned}(1+\alpha)\cos(\lambda\pi)\left[\sin^2\left(\frac{\lambda\pi}{2}\right) - \lambda^2\right] + \frac{1-\alpha}{2}\sin^2(\lambda\pi) \\ \pm f \sin(\lambda\pi)\left\{(1-\alpha)\lambda(1+\lambda) - 2\beta\left[\sin^2\left(\frac{\lambda\pi}{2}\right) - \lambda^2\right]\right\} \\ = 0, \end{aligned} \tag{8}$$

where the positive sign should be taken for trailing-edge slip and the negative sign for leading-edge slip.

In order to determine the critical friction coefficient f_a, below which slip must occur at the corner of a leading edge, from equation (3), we also need the characteristic equation for the eigenvalues $\lambda_i^{(a)}$ for the adhered interface, which is [5, 10]

$$A\beta^2 + B\alpha\beta + C\alpha^2 - B\beta + 2D\alpha + F = 0 \, , \tag{9}$$

where

$$\begin{aligned} A &= 4\left[\sin^2\left(\frac{\lambda\pi}{2}\right) - \lambda^2\right]\sin^2(\lambda\pi) \, ; \\ B &= 4\lambda^2\sin^2(\lambda\pi) \, ; \quad C = \sin^2\left(\frac{\lambda\pi}{2}\right) - \lambda^2 \, ; \\ D &= (2\lambda^2 - 1)\sin^2(\lambda\pi) + \sin^2\left(\frac{\lambda\pi}{2}\right) - \lambda^2 \, ; \\ F &= \sin^2\left(\frac{3\lambda\pi}{2}\right) - \lambda^2 \, . \end{aligned} \tag{10}$$

2.1 Nature of the eigenvalue $\lambda_1^{(s)}$ for edge slip

If Poisson's ratio is restricted to the range $0 \le \nu_1, \nu_2 \le 0.5$, the values of α, β must lie within the parallelograms shown in Fig. 2. These figures show the nature of the first eigenvalue $\lambda_1^{(s)}$ of equation (8) for four different coefficients of friction. In each region, the first term refers to $\lambda_1^{(s)}$ at a trailing edge and the second to that at a leading edge. For example, for the far left region of each figure, $\lambda_1^{(s)}$ is oscillatory and the stress field is bounded [i.e. $\Re(\lambda_1^{(s)}) > 1$] at a trailing edge, and real and singular [$\lambda_1^{(s)} < 1$] at a leading edge.

In region B on the right side of these figures, $\lambda_1^{(s)}$ is real, and the stress field is singular at both edges for all friction coefficients. The eigenvalue is a continuous monotonic function of f, but $\lambda_1^{(s)}$(trailing)$< \lambda_1^{(s)}$(leading) in region B, whereas $\lambda_1^{(s)}$(trailing)$> \lambda_1^{(s)}$(leading) in region A as long as $\lambda_1^{(s)}$ is real. The boundary between these regions is independent of the friction coefficient.

In region A, the characteristics of the eigenvalues depend on the coefficient of friction as well as the material properties, as shown in Fig. 2. The case of similar materials [$\alpha = \beta = 0$] lies within this region, so it is convenient to start by summarizing the behaviour in this case [2, 3], to serve as a reference for the more general case.

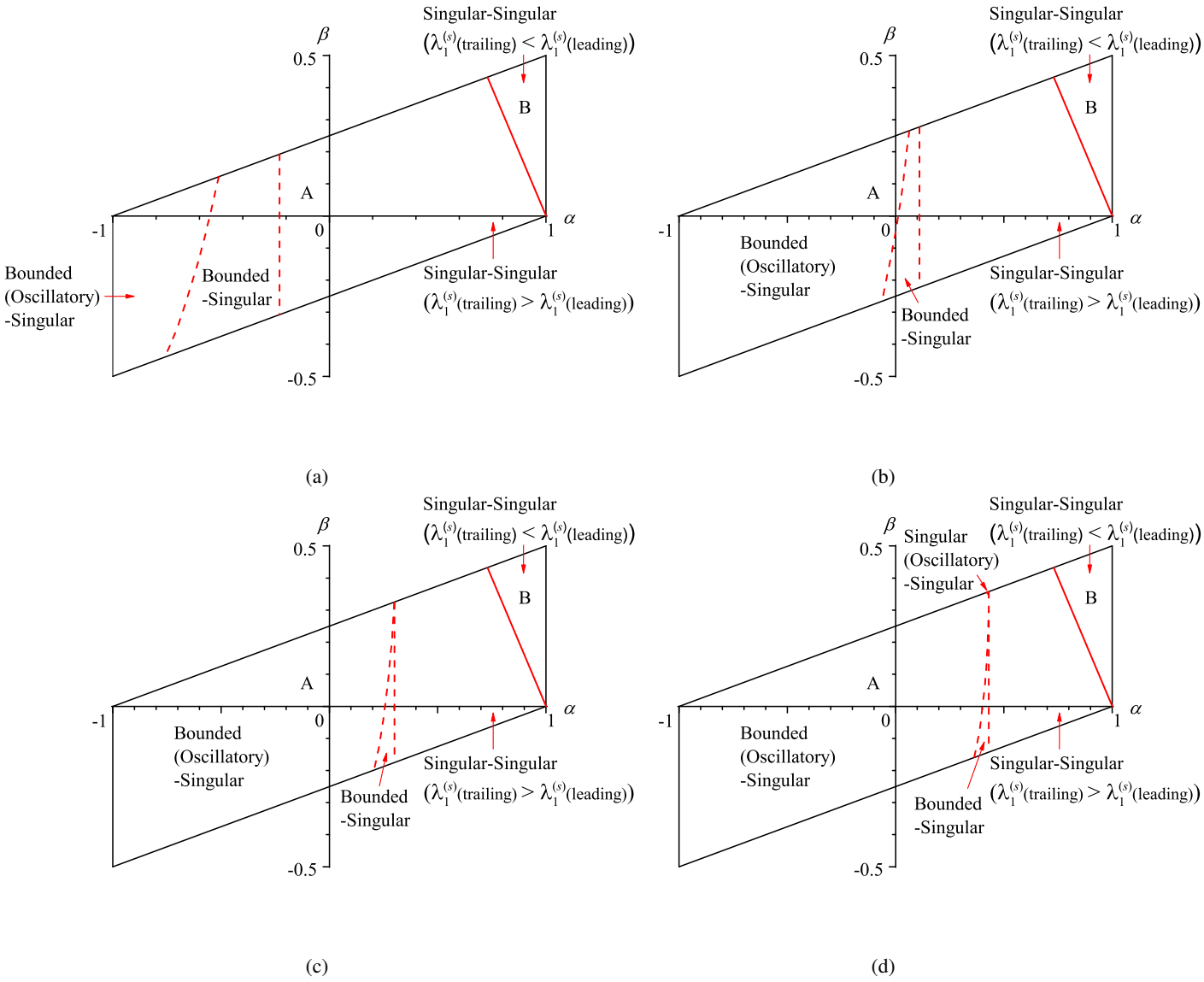

Fig. 2: Characteristics of the first slip eigenvalue $\lambda_1^{(s)}$ [trailing edge – leading edge] with different friction coefficients: (a) $f = 0.2$, (b) $f = 0.4$, (c) $f = 0.6$, (d) $f = 0.8$.

2.2 Similar materials

Figure 3 shows the dependence of the first *slip* eigenvalue $\lambda_1^{(s)}$ on f, including the real and imaginary parts in the range where $\lambda_1^{(s)}$ is complex. In this figure, we identify the critical friction coefficients f_b, f_c and f_a, the last being determined from the eigenfunctions of the adhered equation (9). Recall that f_a characterizes the behaviour of a leading edge and f_b, f_c characterize that of a trailing edge.

At a leading edge, the asymptotic field is always singular and it will involve slip if $f < f_a$. For $f > f_a$, the leading edge must stick [except in the case of gross slip] and the corresponding eigenvalue is determined from equation (9). Notice that if the tangential load is increased towards the gross slip limit with $f > f_a$, the leading edge must remain stuck until this limit is reached, when there will be a discontinuous change to a sliding solution, since the slip eigenvalue is then lower than that for stick. The transition to full sliding was examined by Flicek *et al.* [11] using a finite-element solution.

At a trailing edge, stick is impossible for all values of f and we must have either slip or separation depending on the sign of $K_1^{(s)}$ in the *slip* asymptotic series. In the case of slip, the asymptotic stress field is then singular for $f < f_b$ and bounded for $f_b < f < f_c$. Finally, for $f > f_c$, we always obtain separation in the corner.

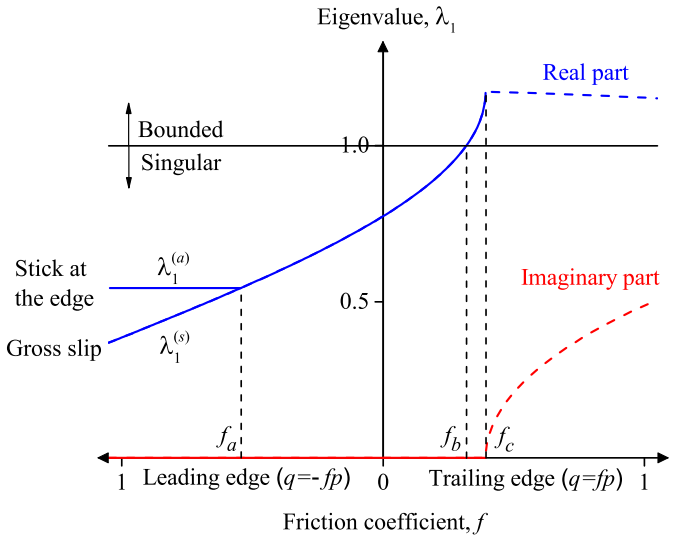

Fig. 3: Lowest eigenvalue .vs friction coefficient for contact between elastically similar materials ($\alpha = \beta = 0$).

2.3 Dissimilar materials

In the more general case of dissimilar materials, the principal effect of the bimaterial parameters α, β is to change the values of the critical friction coefficients f_a, f_b, f_c. However, as long as these three coefficients are defined, the qualitative behaviour of the system remains the same as for similar materials, and all the statements in Section 2.2 remain true. This applies throughout the region labelled A_1 in Fig. 4, where the Dundurs' parallelogram is partitioned depending on the relative magnitudes of the critical friction coefficients in cases where these can be defined.

For material combinations in region A_2, the slip eigenvalue becomes complex before reaching unity, so f_b is not defined. Since f_a and f_c are still defined, the contact edge behaviour is qualitatively similar to that in region A_1, except that in the case of slip, the local stress field is always singular regardless of friction coefficient. Recall that throughout region A $[A_1 \cup A_2]$, $\lambda_1^{(s)}$(trailing)$> \lambda_1^{(s)}$(leading) for $f < f_c$.

In region B, $\lambda_1^{(s)}$ is real and the stress field is singular for all friction coefficients and $\lambda_1^{(s)}$(trailing)$< \lambda_1^{(s)}$(leading). Region B also defines the range of values of (α, β) in which the first eigenvalue of the *adhered* characteristic equation (9) is complex, so for these material combinations, stick at the contact edge is impossible for any coefficient of friction. If the applied loads are insufficient to support gross slip, we then anticipate either a region of edge slip or a region of separation, depending on the sign of $K_1^{(s)}$. A special case is that where body 2 is rigid, giving $\alpha = 1, \beta = (1-2\nu_1)/2(1-\nu_1)$, which defines the right edge of the parallelograms in Fig. 2. The problem of normal indentation of an elastic half-plane by a rigid flat punch was solved by Spence [12], who demonstrated the existence of edge slip zones whose extent depends on both f and β. It is interesting to note that Spence's solution implies that finite [albeit small] slip zones are predicted for arbitrarily large coefficients of friction.

2.3.1 Determination of the critical friction coefficients

In section 2.1, we discussed the nature of the eigenvalues for different coefficients of friction. Here, we determine the critical coefficients of friction for which the nature of the eigenvalues changes.

The critical friction coefficients can be obtained from the characteristic equations (8, 9). For example, f_b is the value at which the first eigenvalue of (8) reaches unity. Since $\lambda = 1$ satisfies this equation for all values of the parameters, we have to apply L'Hôpital's rule, from which we obtain

$$f_b = \frac{1}{\pi}\left(\frac{1+\alpha}{1-\alpha}\right), \tag{11}$$

which we note is independent of β.

The coefficient f_c is the value of f at which the first root of (8) becomes complex, or equivalently at which the first two real roots coincide. It was determined numerically and a contour plot inside the Dundurs' parallelogram is shown in Fig. 5(a).

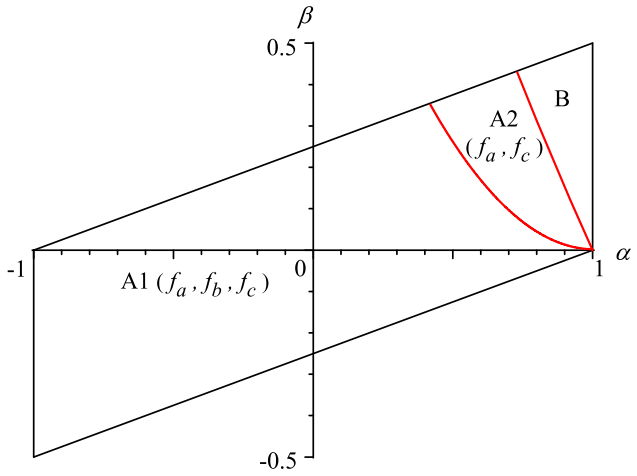

Fig. 4: Partition of the Dundurs parallelogram.

The coefficient f_a can be determined as the ratio of the [adhered] eigenfunctions $f_{\theta r}^{1(a)}(0), f_{\theta\theta}^{1(a)}(0)$ in equation (2). Kim *et al.* [5] used this method to make a contour plot of f_a in the Dundurs parallelogram. This requires calculation of the eigenfunctions and hence entails significant additional algebraic manipulations. However, the case $f = f_a$ essentially represents a pivot between the stick and slip asymptotics, so for this friction coefficient the same functions satisfy both equations (9) and (8). A simpler calculation method is therefore to determine the first eigenvalue from (9), substitute it into the *slip* characteristic equation (8) and then use the resulting equation to solve for f_a. Figure 5(b) shows a contour plot for the magnitude of f_a. We note that both the magnitude of f_a and f_c increase without limit as we approach the boundary between regions A and B.

2.4 Non-monotonic loading

Frictional contact problem are inherently history-dependent in that the current state of a system can depend on the previous loading scenario. The 'memory' of the system resides in the slip displacements locked in any region which transitions from slip or separation to stick [13]. In particular, the detailed history of loading affects the instantaneous state of the system when a slip zone 'advances' into a stick zone [14].

2.4.1 Region A

Suppose that two contacting bodies with material properties corresponding to region A are loaded in such a way that the adhered stress-intensity factors $K_1^{(a)}, K_2^{(a)} < 0$, and $|K_1^{(a)}|$ increases monotonically. For $f < f_a$, as explained in Section 2.3, we anticipate a slip zone near the corner whose size scales with d_0 from equation (4), and for this zone to be non-decreasing we therefore also require that $K_1^{(a)}/K_2^{(a)}$ be non-decreasing. Under these conditions, the embedded field very close to the corner will be described by the leading-edge *slip* asymptotic and the corresponding local normal and tangential tractions can be expressed as equation (5) with the positive sign.

Suppose now that $K_1^{(a)}$ reaches a maximum negative value and then increases by $\Delta K_1^{(a)}$. In many frictional problems, if the tangential loading rate changes sign, the entire interface sticks instantaneously at the maximum load, after which reversed slip zones of growing magnitude are developed. We therefore start with the provisional assumption that the entire contact interface will stick instantaneously in which case the previous tractions would be modified by the adhered asymptotic to

$$\begin{aligned} p(r) &\approx -K_1^{(s)} r^{\lambda_1^{(s)}-1} - \Delta K_1^{(a)} r^{\lambda_1^{(a)}-1} f_{\theta\theta}^{1(a)}(0); \\ q(r) &\approx f K_1^{(s)} r^{\lambda_1^{(s)}-1} + \Delta K_1^{(a)} r^{\lambda_1^{(a)}-1} f_{\theta r}^{1(a)}(0), \end{aligned} \tag{12}$$

where the first term defines the first term in the slip asymptotic series when $K_1^{(a)}$ reaches its maximum negative value. Since $\lambda_1^{(s)} > \lambda_1^{(a)}$, the contact edge behaviour is dominated by the $\Delta K_1^{(a)}$ term and therefore the edge separates $[\Delta K_1^{(a)} > 0]$ with

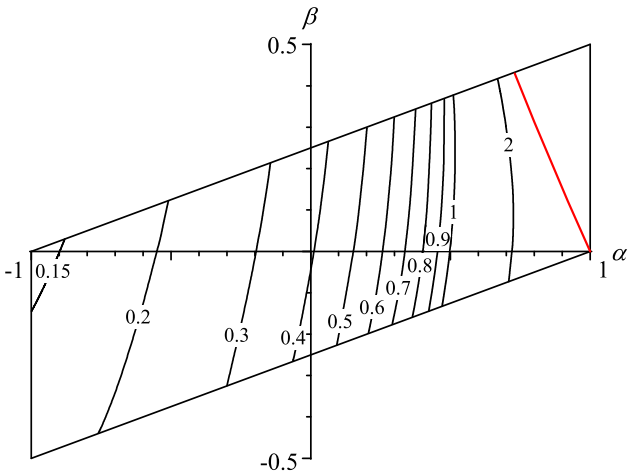

(a)

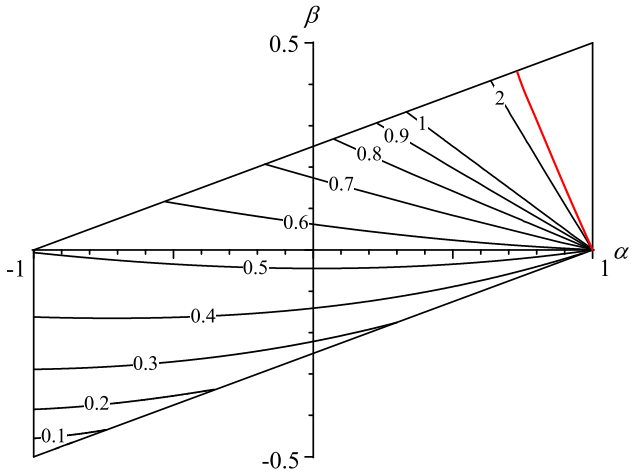

(b)

Fig. 5: Contour plots of the critical friction coefficients: (a)f_c, (b)f_a.

an adjacent 'trailing-edge' slip zone [2]. The sizes of these zones will vary continuously with ΔK_1 and by analogy with (4) should scale with

$$d_1 = \left(\frac{\Delta K_1^{(a)}}{K_1^{(s)}} \right)^{1/(\lambda_1^{(s)} - \lambda_1^{(a)})} . \tag{13}$$

We next consider the case where $K_1^{(a)}$ is negative and decreases monotonically, but $K_1^{(a)}/K_2^{(a)}$ reaches a maximum and then decreases. Equation (4) would then imply a decrease in d_0 and hence in the extent of the slip zone, but this defines a state of advancing stick, where we expect the solution to depend on the precise relation between $K_1^{(a)}$ and $K_2^{(a)}$ during this phase of the loading. Problems of this kind can only be solved using an incremental formulation.

2.4.2 Region B

For material combinations in region B, the first eigenvalue $\lambda_1^{(a)}$ and stress-intensity factor $K_1^{(a)}$ are complex, implying oscillatory fields at the corner, which violate both the frictional and Signorini inequalities. We anticipate a small region of leading-edge slip adjacent to the corner, embedded in the surrounding oscillatory asymptotic field. The extent of this region will remain constant if $|K_1^{(a)}|$ increases monotonically and $\arg\{K_1^{(a)}\}$ remains constant. The extent of the slip zone is a monotonic function of $\arg\{K_1^{(a)}\}$ and hence this solution also remains valid if $\arg\{K_1^{(a)}\}$ increases monotonically. As in Section 2.4.1, the tractions very close to the corner can then be characterized by the first term in the slip asymptotic.

If $\arg\{K_1^{(a)}\}$ is constant and $|K_1^{(a)}|$ increases monotonically to a maximum and then decreases, we again assume instantaneous stick, leading to tractions of the form (12), except that the contribution from $\Delta K_1^{(a)}$ is now oscillatory. However, $\Re\{\lambda_1^{(a)}\} < \lambda_1^{(s)}$(leading) for all $f > 0$ [they are equal for $f = 0$] so the change in the field is dominated by $\Delta K_1^{(a)}$ and we therefore anticipate a region of separation at the corner and an adjacent region of trailing-edge slip.

Turner [15] considered the problem where an axisymmetric rigid flat punch is pressed into an elastic half space by a normal force which is first increased to a maximum value and then decreased. During the monotonic loading phase, Spence [12] determined the [constant] size of the leading edge slip zone as a function of f and β. During unloading, Turner found that leading-edge slip penetrated further away from the edge, but was surrounded by an annulus of stick until the normal load had been reduced to about half its maximum value, after which a further annulus of trailing-edge slip is developed. This conclusion violates the present asymptotic arguments, since we now know that stick at the corner is impossible under any loading conditions. We must conclude that Turner's numerical solution was insufficiently refined to detect the inevitable small regions of slip and separation once unloading commences.

3 Conclusion

In this paper, we have investigated the influence of material dissimilarity on the corner traction fields for contact between an elastic right-angle wedge and an elastic half-plane. The material parameters define a point in the Dundurs parallelogram of Fig. 4 and qualitatively distinct behaviour is predicted depending on whether this point lies in region A or region B of this figure.

For material combinations in region A, the behaviour is qualitatively similar to that for the case where the materials are the same, but the critical friction coefficients identified by Karuppanan *et al.* [3] and Churchman and Hills [2] are changed. Contour plots of these coefficients are presented in Fig. 5.

For material combinations in region B, the behaviour is qualitatively similar to that for the case where the wedge is rigid and the half-plane is elastic. If an initial period of monotonic loading is followed by a load reversal, the initial behaviour can be predicted based on the relative strengths of the singularities associated with the locked-in shear tractions and the incremental stick asymptotic.

The results give insight into the high local stresses at the edge of a contact between elastically dissimilar bodies, such as those involved in PCI failure [6]. They can also be used to evaluate corresponding finite element models, in particular to determine whether the mesh is sufficiently refined near the corner to recover the appropriate analytically predicted asymptotic behaviour.

Acknowledgements

This research was supported by the Consortium for Advanced Simulation of Light Water Reactors (http://www.casl.gov), an Energy Innovation Hub (http://www.energy.gov/hubs) for Modeling and Simulation of Nuclear Reactors under U.S. Department of Energy Contract No. DE-AC05-00OR22725.

References

[1] Williams, M.L., 1952. "Stress singularities resulting from various boundary conditions in angular corners of plates in extension". *J. Appl. Mech.*, **19**(4), pp.526–528.

[2] Churchman, C.M. and Hills, D.A., 2006. "General results for complete contacts subject to oscillatory shear". *J. Mech. Phys. Solids*, **54**(6), pp.1186–1205.

[3] Karuppanan, S., Churchman, C.M., Hills, D.A. and Giner, E., 2008. "Sliding frictional contact between a square block and an elastically similar half-plane". *Eur. J. Mech.*, **27**(3), pp.443–459.

[4] Churchman, C.M. and Hills, D.A., 2006. "Slip zone length at the edge of a complete contact". *Int. J. Solids Struct.*, **43**(7-8), pp.2037–2049.

[5] Kim, H.K., Hills, D.A. and Paynter, R.J., 2014. "Asymptotic analysis of an adhered complete contact between elastically dissimilar materials". *Journal of Strain Analysis*, **49**(8), pp.607–617.

[6] Cox, B., 1990. "Pellet-clad interaction (PCI) failures of zirconium alloy fuel claddinga review". *J. Nucl. Mater.*, **172**(3), pp.249–292.
[7] Dundurs, J., 1969. "Discussion of edge-bonded dissimilar orthogonal elastic wedges under normal and shear loading". *J. Appl. Mech.*, **36**(3), pp.650–652.
[8] Gdoutos, E.E. and Theocaris, P.S., 1975. "Stress concentrations at the apex of a plane indenter acting on an elastic half-plane". *J. Appl. Mech.*, **42**(3), pp.688–692.
[9] Comninou, M., 1976. "Stress singularity at a sharp edge in contact problems with friction". *Zeitschrift für Angew. Math. und Phys. ZAMP*, **27**(4), pp.493–499.
[10] Bogy, D.B., 1971. "Two edge-bonded elastic wedges of different materials and wedge angles under surface tractions". *J. Appl. Mech.*, **38**(2), pp.377–386.
[11] Flicek, R.C., Ramesh, R. and Hills, D.A., 2015. "A complete frictional contact: the transition from normal load to sliding". *Int. J. Eng. Sci.*, **92**, pp.18–27.
[12] Spence, D.A., 1973, "An eigenvalue problem for elastic contact with finite friction". *Proceedings of the Cambridge Philosophical Society*, **73**(1), pp. 249–268.
[13] Barber, J.R., Davies, M. and Hills, D.A., 2011. "Frictional elastic contact with periodic loading". *Int. J. Solids Struct.*, **48**(13), pp.2041–2047.
[14] Comninou, M. and Dundurs, J., 1982. "An Educational Elasticity Problem with Friction, Part 2: Unloading for Strong Friction and Reloading". *J. Appl. Mech.*, **49**(1), pp.47–51.
[15] Turner, J.R., 1979. "The frictional unloading problem on a linear elastic half-space". *IMA J. Appl. Math.*, **24**(4), pp.439–469.